2021 43rd Annual International Conference of the
IEEE Engineering in Medicine & Biology Society (EMBC)
Oct 31 - Nov 4, 2021. Virtual Conference

Examining the Influence of Spatial Smoothing on Spatiotemporal Features of Intrinsic Connectivity Networks at Low ICA Model Order

Behnaz Jarrahi, *Member, IEEE*

***Abstract*— Using a relatively high model order of independent component analysis (ICA with 75 ICs) of functional magnetic resonance imaging (fMRI) data, we have reported a clear effect of spatial smoothing Gaussian kernel size on spatiotemporal properties of intrinsic connectivity networks (ICNs). However, many if not the majority of ICA fMRI studies are usually performed at low model order, e.g., 20-IC decomposition, as such low order is generally enough to extract the few networks of interest such as the default-mode network (DMN). The aim of this study is to investigate if we can replicate the spatial smoothing effects on spatiotemporal features of ICNs at low ICA model order. Same resting state fMRI data that we used with 75-IC analysis were used here. Spatial smoothing using an isotropic Gaussian filter kernel with full width at half maximum (FWHM) of 4, 8, and 12 mm was applied during preprocessing. ICNs were identified from 20-IC decomposition and evaluated in terms of three primary features: spatial map intensity, functional network connectivity (FNC), and power spectra. The results identified similar effects of spatial smoothing on spatial map intensities and power spectra at $p < 0.01$, false discovery rate (FDR) corrected for multiple comparisons. Reduced spatial smoothing kernel size resulted in decreased spatial map intensities as well as a generally decreased low-frequency power (0.01 – 0.10 Hz) but increased high-frequency power (0.15 – 0.25 Hz). FNC, however, did not show a uniform change in correlation values with the size of smoothing kernel. Notably, FNC between DMNs decreased but FNC between central executive and visual networks increased with an increase in smoothing kernel size. These preliminary findings confirm spatial smoothing influences ICN features regardless of model order. The discussion focuses on differences between observed changes at low and high ICA model orders.**

I. INTRODUCTION

Earlier studies indicate that preprocessing methods that are commonly used prior to the analysis of the functional magnetic resonance imaging (fMRI) may affect the properties of brain networks [1], [2]. For example, Lui and colleagues showed that large smoothing kernel may cause a correlation-based functional overestimation [3]. In a series of resting state studies that we are presenting along with this paper, we meticulously examined different features of brain intrinsic connectivity networks (ICNs) following a well-established independent component analysis (ICA) at relatively high model order of 75-IC [4]. Our results revealed that the level of spatial smoothing clearly affects the spatial maps, functional network connectivity (FNC [5]), and power spectra. Considering that most ICA studies are performed on low model order of, e.g., 20, the aim of the present study was to determine whether our findings can be replicated for data analyzed at low ICA model order.

B. Jarrahi is with the Department of Anesthesia, Stanford University, CA, USA; (email: behnaz.jarrahi@stanford.edu).

II. MATERIALS AND METHODS

A. Data Acquisition and Preprocessing

This study was conducted on existing resting state data from 22 healthy right-handed subjects (ten males, twelve females, average age 37.73 years) who were scanned with a 3.0 T MRI scanner with an 8-channel receive-only RF head coil array (Discovery MR750, GE Medical Systems, Milwaukee, WI, USA). BOLD fMRI data were acquired using EFGRE3D pulse sequence (TR = 2s, TE = 30 ms, flip angle = 76^o, acquisition matrix = 64×64, field of view (FOV) = 220×220 mm^2, slice thickness = 4 mm, gap = 1 mm, total number of slices = 31 slices, 360 volumes, ascending acquisition). Subjects were instructed to remain calm and awake as they rested with their eyes closed and refrain from sleeping. Informed consent was obtained from all subjects according to institutional guidelines at the Stanford University, and all data were anonymized prior to group analysis. None of the subjects had a history of neurological or psychiatric disorders or metal implants in the body. Following MR image quality assessment in MRIQC (Stanford University, USA) [6], data were preprocessed using SPM12b (Wellcome Department of Cognitive Neurology, UCL, UK). Preprocessing pipeline included motion and slice time correction, and spatial normalization into the Montreal Neurological Institute (MNI) reference space. Data were then spatially smoothed using a Gaussian kernel with a full-width at half-maximum (FWHM) of 4, 8, and 12 mm. FWHM of 8 mm was chosen as it is the typical value used in group ICA fMRI studies, and FWHM of 4 mm and 12 mm were considered as arbitrary low and high smoothing values.

B. Independent Component Analysis and Post-processing

Group ICA was performed in three steps using the GIFT toolbox (GroupICAT v4.0c, University of New Mexico, USA). In the first step, subject-specific data reduction principal component analysis (PCA) with a standard economy-size decomposition retained 30 PCs. In the second step, data were concatenated across time and group data reduction with expectation-maximization algorithm retained 20 PCs. Infomax ICA algorithm [7] was used and repeated 20 times with random initiation in ICASSO [8], and estimated group-level ICs were back-reconstructed using GICA3 method. ICNs were identified from artifactual components following the methodology recommended by Allen et al. [4]. Prior to connectivity analysis (see below), time-courses were detrended, despiked with AFNI's 3dDespike and bandpass filtered at [0.01 – 0.15] Hz.

Table 1. ICN Sptial Map Information

ICN	IC#	Iq	4 mm						8 mm						12 mm					
			Vol (vox)	Tmax	x	y	z	Peak	Vol (vox)	Tmax	x	y	z	Peak	Vol (vox)	Tmax	x	y	z	Peak
VN	IC02	0.976	6112	13.32	6	-58	-10	Cerebellar Vermis (4/5)	14617	16.8	-12	-68	26	L Cuneus	21155	22.68	16	-74	-2	R Lingual Gyrus
SMN	IC10	0.970	4780	13.58	52	-12	28	R Postcentral Gyrus	14568	14.84	56	8	28	R IFG (p. Opercularis)	21350	20.58	62	-12	16	R Postcentral Gyrus
	IC15	0.958	2012	11.2	-8	-54	70	L Precuneus	11469	18.14	-2	-34	84	L Postcentral Gyrus	19774	25.98	-20	-38	66	L Postcentral Gyrus
DMN	IC06	0.980	15126	19.5	4	-40	28	R PCC	25968	23.75	2	-24	32	R MCC	38205	27.73	6	-58	18	R Precuneus
	IC08	0.971	10930	17.42	-2	44	12	L ACC	19875	30.58	-4	52	6	L Superior Medial Gyrus	31042	45.78	-4	50	8	L ACC
SRN	IC14	0.949	4723	16.21	-12	42	8	L ACC	13470	21.72	8	38	4	R ACC	21968	23.55	10	36	2	R ACC
SN	IC05	0.984	21714	25.16	-32	-10	-6	L Putamen	32982	35.2	-30	4	4	L Putamen	43263	40.08	-30	4	6	L Putamen
CEN	IC03	0.981	9007	16.08	-48	32	-6	L IFG (p. Orbitalis)	18210	19.38	-34	50	-10	L Middle Orbital Gyrus	29189	24.85	-36	50	-8	L Middle Orbital Gyrus
	IC04	0.976	10260	17.64	36	30	40	R Middle Frontal Gyrus	18362	17.53	22	58	-6	R Superior Orbital Gyrus	29957	23.21	22	60	-6	R Superior Orbital Gyrus
DAN	IC18	0.937	3771	14.99	-10	-70	52	L Precuneus	13067	22.62	-10	-70	52	L Precuneus	20998	29.89	10	-60	56	R Precuneus

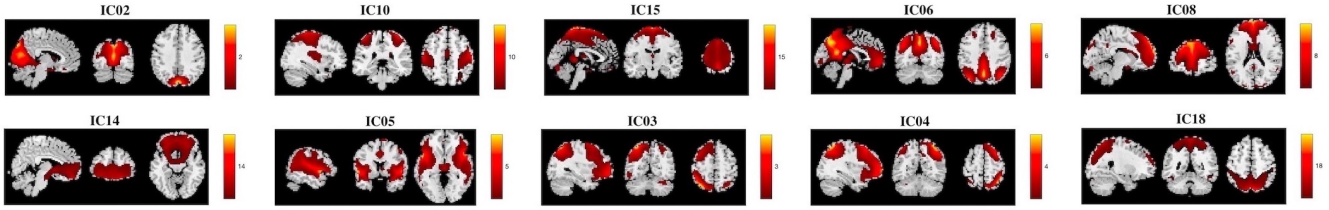

Fig. 1. Spatial maps of 10 ICNs from 20-IC decomposition are shown in neurological convention (right is right).

C. ICN Feature Analyses

To define significant brain regions associated with each ICN, back-reconstructed spatial maps was normalized into z scores. Next, the z score averaged maps were entered into second level random effects analysis in SPM12b [9]. Significance threshold was set at $p < 0.05$ family-wise error (FWE) corrected for multiple comparisons of voxel-wise whole-brain analysis. Number of voxels, and the highest-value and the locus of the peak activation (x, y, z) in MNI coordinates were saved. Functional network connectivity (FNC [5]) was performed on IC time courses using the MANCOVAN toolbox in GIFT by computing Pearson's correlation values between pairwise ICNs. Fisher r-to-z transformation was applied to normalize the FNC correlation values [4]. Power spectra were computed for each subject's time-courses and separately for each smoothing condition on full range of the frequency bands, i.e., [0 – 0.25] Hz. To determine which spatial map voxels, FNC correlations or spectral bins were influenced by spatial smoothing kernel size, pairwise paired t-test was performed at the false discovery rate [FDR]-corrected threshold of 0.01. Significant effects were visualized by plotting the log of p-value with the inverse sign of the associated t-statistic, i.e., $-sign(t)log_{10}(p)$ to provide better information on directionally and statistical strength [4].

III. RESULTS

From 20-IC decomposition, ten ICs were identified as ICNs (Fig. 1). They included a visual network (VN; IC02), two sensorimotor networks (SMN; ICs 10 and 15), two default mode networks (DMN; ICs 30 and 34), self-referential network (SRN, IC14), salience network (SN, IC05), two frontoparietal central executive networks (CENs; ICs 3 and 4), and dorsal attention network (DAN, IC18) [10]–[14]. Number of voxels in each FWE-thresholded ICN spatial maps, MNI (x, y, z) location of the peak voxel and associated t-score are provided for each smoothing condition in Table 1. Note that the peak location and t-values are not identical between different smoothing condition. Results summarizing the effects of smoothing kernel FWHM size on spatial map intensities are shown in Fig. 2 (FDR-corrected $p < 0.01$). Due to the importance of DMN and SN especially in resting state studies (such as in interoception studies [15]–[17]), significant differences in intensities of DMN and SN spatial maps for different pairwise paired t-test (S4 – S8, S8 – S12, S4 – S12, where S stands for smoothing kernel FWHM sizes of 4, 8, or 12 mm) are shown separately in Fig. 3. FNC correlations averaged over subjects for each smoothing condition, and significant differences in FNC between conditions are shown in Figs. 4A and 4B, respectively. The effects of smoothing on ICN power spectra are displayed in Fig. 5 (FDR-corrected $p < 0.01$).

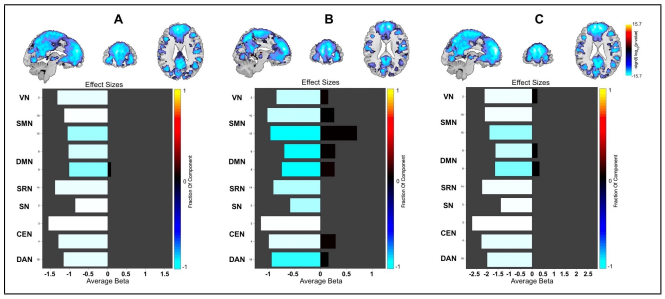

Fig. 2. Significant effects of smoothing on spatial maps. Results of paired t-test are shown for **A** S4 – S8, **B** S8 – S12, and **C** S4 – S12, where S denotes smoothing kernel sizes of 4, 8, or 12 mm. FDR-corrected $p < 0.01$.

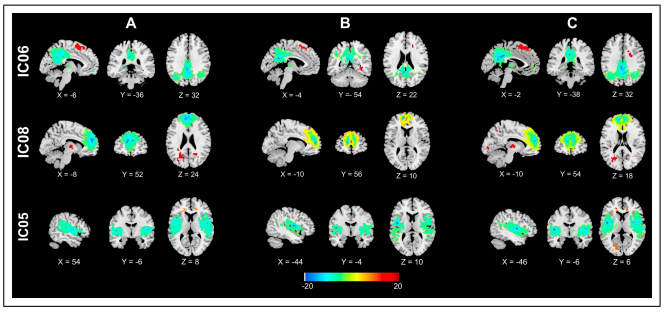

Fig. 3. Significant effects of smoothing on DMN and SN spatial maps. Results of paired t-test are shown for **A** S4 – S8, **B** S8 – S12, and **C** S4 – S12, where S = FWHM 4, 8, or 12 mm. FDR-corrected $p < 0.01$.

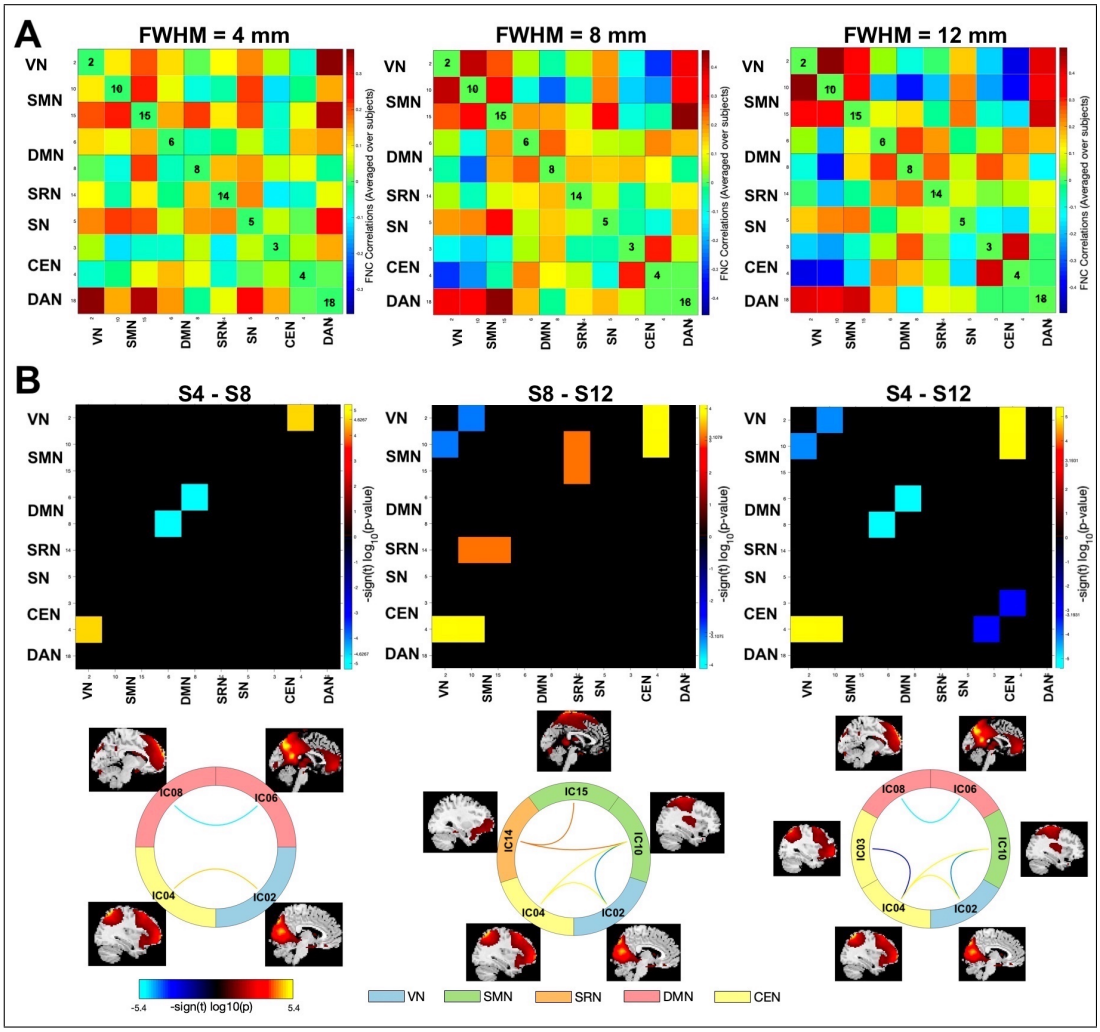

Fig. 4. **A** FNC correlation matrices for smoothing kernel FWHM of 4, 8, or 12 mm; **B** Significant differences in FNC correlations for different pairwise paired t-test, where S stands for smoothing kernel FWHM. For each paired t-test, results are shown for all ICNs (top), and as connectogram (bottom). FDR-corrected $p < 0.01$.

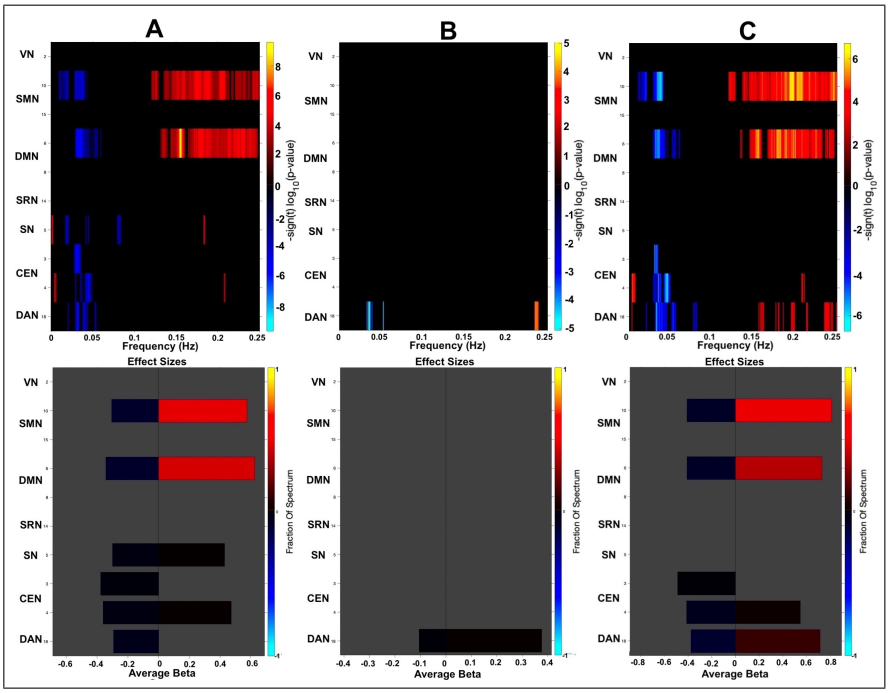

Fig. 5. Significant effects of smoothing kernel sizes on power spectra. **A** S4 – S8, **B** S8 – S12, and **C** S4 – S12, where S is smoothing kernel FWHM of 4, 8, or 12 mm. T-maps of significant effects are shown as composite t-maps. Beta-values are averaged over significant clusters. FDR-corrected $p < 0.01$.

IV. Discussion

Similar to other studies that used low-level ICA model order to extract ICNs from fMRI data, we could successfully identify well-known ICNs with sufficient spatial segregation of functional regions in our data. From 20 components, we identified 10 ICNs that are highly reminiscent of those described in previous studies [10]–[16]. As we showed in previous study of low vs. high ICA model order [18], not all ICN types appeared in this low-order decomposition. For example, ventral attention network or subcortical networks were not present here.

After performing pairwise paired *t*-test on data that were preprocessed using three different spatial smoothing kernel sizes, we found mostly similar effects of smoothing on ICN features as we reported for 75-IC model order. There was a decrease in spatial maps of all ICNs with a reduction in the smoothing kernel size. Number of voxels in each FWE-thresholded ICN spatial maps, location of the peak voxel and associated *t*-score were also changed with the smoothing kernel sizes. There was a reduction in volume of networks and *t*-score with smaller smoothing kernel sizes. In addition, similar to high-level ICA, power spectra analysis of low-level ICA showed generally increased high-frequency power (0.15 – 0.25 Hz) but decreased low-frequency power (0.01 – 0.10 Hz) with a decrease in the smoothing kernel size.

FNC of low model order ICA with FDR-corrected *p*-value of 0.01 (Fig. 4A), also showed general reduction in the between-network connectivity (FNC correlations) in particular between the dorsal and ventral DMN (S4 – S8, and S4 – S12, with S denoting smoothing kernel FWHM), and to a lesser degree between the VN and SMN (S8 – S12, and S4 – S12), and between the CEN and DAN with smaller smoothing kernel sizes. There were few exceptions. The FNC involving the CEN and VN and sometimes SMN showed strengthening with the reduction of smoothing kernel size. In our FNC findings of high order ICA, we have shown that smaller smoothing kernel influenced the between-network connectivity strength by generally decreasing the FNC correlations. This effect was shared among most ICNs. However, upon revisiting the FNC results and comparing it to low-level model ICA finding here, we spot similar trend in FNC increase involving CEN and other cognitive/attention networks with reduction in smoothing kernel size. But after averaging between networks at high-level ICA, this effect did not survive the stringent FDR-corrected p-value of 0.01.

V. Conclusion

ICA-based network analysis is gaining momentum in fMRI studies. The findings that we reported in this and other accompanying papers provide a preliminary observation on how smoothing kernel size influence different spatiotemporal features of functional brain networks at low and high-model order ICA of resting state fMRI data. For further understanding of these effects, more research with larger data sample is needed to study how preprocessing variances associated with smoothing may influence ICA outcomes.

References

[1] T. Alakörkkö, H. Saarimäki, E. Glerean, J. Saramäki, and O. Korhonen, "Effects of spatial smoothing on functional brain networks," *European Journal of Neuroscience*, vol. 46, no. 9, pp. 2471–2480, 2017.

[2] A. Gardumi, D. Ivanov, L. Hausfeld, G. Valente, E. Formisano, and K. Uludağ, "The effect of spatial resolution on decoding accuracy in fmri multivariate pattern analysis," *Neuroimage*, vol. 132, pp. 32–42, 2016.

[3] P. Liu, V. Calhoun, and Z. Chen, "Functional overestimation due to spatial smoothing of fmri data," *Journal of neuroscience methods*, vol. 291, pp. 1–12, 2017.

[4] E. A. Allen, E. B. Erhardt, Damaraju, *et al.*, "A baseline for the multivariate comparison of resting-state networks," *Frontiers in systems neuroscience*, vol. 5, 2011.

[5] M. J. Jafri, G. D. Pearlson, M. Stevens, and V. D. Calhoun, "A method for functional network connectivity among spatially independent resting-state components in schizophrenia," *Neuroimage*, vol. 39, no. 4, pp. 1666–1681, 2008.

[6] O. Esteban, D. Birman, M. Schaer, O. O. Koyejo, R. A. Poldrack, and K. J. Gorgolewski, "Mriqc: Advancing the automatic prediction of image quality in mri from unseen sites," *PloS one*, vol. 12, no. 9, 2017.

[7] A. J. Bell and T. J. Sejnowski, "An information-maximization approach to blind separation and blind deconvolution," *Neural computation*, vol. 7, no. 6, pp. 1129–1159, 1995.

[8] J. Himberg and A. Hyvarinen, "Icasso: software for investigating the reliability of ica estimates by clustering and visualization," in *2003 IEEE XIII Workshop on Neural Networks for Signal Processing (IEEE Cat. No. 03TH8718)*. IEEE, 2003, pp. 259–268.

[9] B. Jarrahi, D. Mantini, and S. Kollias, "Effect of interoception on intra-and inter-network connectivity of human brain—an independent component analysis of fmri data," in *2015 7th International IEEE/EMBS Conference on Neural Engineering (NER)*. IEEE, 2015, pp. 320–323.

[10] A. R. Laird, P. M. Fox, S. B. Eickhoff, J. A. Turner, *et al.*, "Behavioral interpretations of intrinsic connectivity networks," *Journal of cognitive neuroscience*, vol. 23, no. 12, pp. 4022–4037, 2011.

[11] M. E. Raichle, A. M. MacLeod, A. Z. Snyder, W. J. Powers, D. A. Gusnard, and G. L. Shulman, "A default mode of brain function," *Proceedings of the National Academy of Sciences*, vol. 98, no. 2, pp. 676–682, 2001.

[12] B. Jarrahi and D. Mantini, "The nature of the task influences intrinsic connectivity networks: An exploratory fmri study in healthy subjects," in *2019 9th International IEEE/EMBS Conference on Neural Engineering (NER)*. IEEE, 2019, pp. 489–493.

[13] W. W. Seeley, V. Menon, A. F. Schatzberg, J. Keller, G. H. Glover, H. Kenna, A. L. Reiss, and M. D. Greicius, "Dissociable intrinsic connectivity networks for salience processing and executive control," *The Journal of neuroscience*, vol. 27, no. 9, pp. 2349–2356, 2007.

[14] S. M. Smith, P. T. Fox, K. L. Miller, D. C. Glahn, P. M. Fox, C. E. Mackay, N. Filippini, K. E. Watkins, R. Toro, A. R. Laird, *et al.*, "Correspondence of the brain's functional architecture during activation and rest," *Proceedings of the National Academy of Sciences*, vol. 106, no. 31, pp. 13 040–13 045, 2009.

[15] B. Jarrahi and S. Kollias, "Impact of intravesical cold sensation on functional network connectivity estimated using ica at rest & during interoceptive task," in *2020 42nd Annual International Conference of the IEEE Engineering in Medicine & Biology Society (EMBC)*. IEEE, 2020, pp. 1722–1725.

[16] B. Jarrahi, D. Mantini, J. H. Balsters, L. Michels, T. M. Kessler, U. Mehnert, and S. S. Kollias, "Differential functional brain network connectivity during visceral interoception as revealed by independent component analysis of fmri time-series," *Human brain mapping*, vol. 36, no. 11, pp. 4438–4468, 2015.

[17] B. Jarrahi and S. Kollias, "Effects of visceral interoception on topological properties of the brain–a graph theory analysis of resting state fmri," in *2020 42nd Annual International Conference of the IEEE Engineering in Medicine & Biology Society (EMBC)*. IEEE, 2020, pp. 1116–1119.

[18] B. Jarrahi and D. Mantini, "Hierarchical subdivision and effect of ica model dimensionality on the interoceptive task-derived brain networks," in *2016 IEEE-EMBS International Conference on Biomedical and Health Informatics (BHI)*. IEEE, 2016, pp. 57–61.